

Enhanced Antitumor Efficacy of Vasculostatin (Vstat120) Expressing Oncolytic HSV-1

Jayson Hardcastle^{1,2}, Kazuhiko Kurozumi^{1,*}, Nina Dmitrieva¹, Martin P Sayers^{1,3}, Sarwat Ahmad⁴, Peter Waterman^{5,6}, Ralph Weissleder^{5,6}, E Antonio Chiocca¹ and Balveen Kaur¹

¹Dardinger Laboratory for Neuro-oncology and Neurosciences, Department of Neurological Surgery, James Comprehensive Cancer Center and The Ohio State University Medical Center, Columbus, Ohio, USA; ²Integrated Biomedical Sciences Graduate Program, The Ohio State University Medical Center, Columbus, Ohio, USA; ³Undergraduate Major in Biomedical Science, The Ohio State University Medical Center, Columbus, Ohio, USA; ⁴College of Medicine, The Ohio State University Medical Center, Columbus, Ohio, USA; ⁵Center for Molecular Imaging Research, Massachusetts General Hospital, Charlestown, Massachusetts, USA; ⁶Center for Systems Biology, Massachusetts General Hospital, Boston, Massachusetts, USA

Oncolytic viral (OV) therapy is a promising therapeutic modality for brain tumors. Vasculostatin (Vstat120) is the cleaved and secreted extracellular fragment of brain-specific angiogenesis inhibitor 1 (BAI1), a brain-specific receptor. To date, the therapeutic efficacy of Vstat120 delivery into established tumors has not been investigated. Here we tested the therapeutic efficacy of combining Vstat120 gene delivery in conjunction with OV therapy. We constructed RAMBO (Rapid Antiangiogenesis Mediated By Oncolytic virus), which expresses Vstat120 under the control of the herpes simplex virus (HSV) IE4/5 promoter. Secreted Vstat120 was detected as soon as 4 hours postinfection *in vitro* and was retained for up to 13 days after OV therapy in subcutaneous tumors. RAMBO-produced Vstat120 efficiently inhibited endothelial cell migration and tube formation *in vitro* ($P = 0.0005$ and $P = 0.0184$, respectively) and inhibited angiogenesis ($P = 0.007$) *in vivo*. There was a significant suppression of intracranial and subcutaneous glioma growth in mice treated with RAMBO compared to the control virus, HSVQ ($P = 0.0021$ and $P < 0.05$, respectively). Statistically significant reduction in tumor vascular volume fraction (VVF) and microvessel density (MVD) was observed in tumors treated with RAMBO. This is the first study to report the antitumor effects of Vstat120 delivery into established tumors and supports the further development of RAMBO as a possible cancer therapy.

Received 22 January 2009; accepted 5 September 2009; published online 20 October 2009. doi:10.1038/mt.2009.232

INTRODUCTION

Glioblastoma multiforme is the most common and malignant form of brain tumors, and even after decades of research, the median survival of patients treated with radiation and chemotherapy remains <15 months.¹ Despite the molecular heterogeneity of genetic alterations observed in malignant gliomas, increased vascularity and microvascular proliferation remain one of its

histopathologic hallmarks. The concept of using antiangiogenic strategies to block tumor vasculature as a therapeutic strategy for glioma is currently being tested in human patients.² Although these studies have yielded encouraging results, it is becoming increasingly obvious that a multipronged therapeutic approach combining antiangiogenic agents with cytotoxic agents will be essential to combat this deadly disease.

Another promising new direction in cancer therapy is the use of oncolytic viruses (OV), which exploit tumor-specific conditions to infect and/or replicate in cancer cells leading to their oncolytic destruction.³ Phase I/II clinical testing of OV has demonstrated the relative safety of this approach in human patients up to doses of 10^9 plaque-forming units (pfu) with no therapy-associated toxicity or adverse events.^{4,5} Future large randomized phase III clinical trials will evaluate therapeutic efficacy of this approach.

One of the major limitations in OV therapy is the rapid innate immune responses initiated in tumors upon infection. This antiviral immune response is accompanied by the secretion of several proangiogenic factors^{6–11} that can induce angiogenesis and encourage growth of residual tumor after viral clearance. Corneal infection of wild-type herpes simplex virus type 1 (HSV-1) has also been linked to increased expression of angiogenic factors, such as vascular endothelial growth factor, matrix metalloproteinase 9, Cox-2, and reduced expression of antiangiogenic factors, such as thrombospondin 1 (TSP-1) and TSP-2 (refs. 11,12). Consistent with these studies, we and others have recently reported a significant increase in cysteine-rich 61 (CYR61), and reduction of antiangiogenic TSP-1 after oncolytic HSV-1 treatment.^{11,12} CYR61-mediated $\alpha_v\beta_5$ (ref. 13) integrin activation and reduced TSP-1 (antiangiogenic ligand for CD36 on endothelial cells) levels have been implicated in increased angiogenesis of the residual tumor that regrows following OV-mediated tumor destruction and viral clearance.¹⁴

Vasculostatin (Vstat120) is the extracellular fragment of brain-specific angiogenesis inhibitor 1 (BAI1), and has been shown to be a potent antiangiogenic and antitumorogenic factor. Vstat120 contains five TSP type 1 repeats (amino acids 264–315, 357–407, 412–462, 470–520, and 525–575) and an integrin-antagonizing

*Current address: Department of Neurological Surgery, Okayama University Graduate School of Medicine, Okayama, Japan.

Correspondence: Balveen Kaur, Department of Neurological Surgery, Dardinger Laboratory for Neuro-oncology and Neurosciences, The Ohio State University, 385-D OSUCCC, 410 West 12th Avenue, Columbus, Ohio 43210, USA. E-mail: Balveen.Kaur@osumc.edu

RGD motif (amino acids 231–233) (ref. 15). Both the TSRs as well as the RGD integrin-binding domains of BAI1 have been shown to have antiangiogenic functions.^{16,17} The RGD integrin-binding motif of BAI1 has been shown to be angiostatic by antagonizing activation of $\alpha_v\beta_5$ family of integrins.¹⁸ The five TSP1 domains of Vstat120 have also been shown to be antiangiogenic *in vitro* and *in vivo*.^{19,20} Although armed oncolytic HSV-1-derived viruses expressing a variety of angiostatic factors have been described,^{21–25} we hypothesized that efficient production of Vstat120 expressed under the IE4/5 HSV promoter would counter the reduction of TSP-1 and increased CYR61 integrin activation in the glioma microenvironment thereby leading to enhanced anti glioma efficacy of OV (Figure 1).

We have created an armed oncolytic HSV-1 that expresses Vstat120 under the expression of an immediate early IE4/5 HSV promoter. Based on the potent and rapid induction of antiangiogenic Vstat120, we named this virus RAMBO (Rapid Antiangiogenesis Mediated By Oncolytic virus). Treatment of mice bearing intracranial and subcutaneous gliomas revealed a significant increase in antitumor efficacy of RAMBO compared to the control HSVQ virus. This is the first study to investigate therapeutic efficacy of Vstat120 delivery in established tumors.

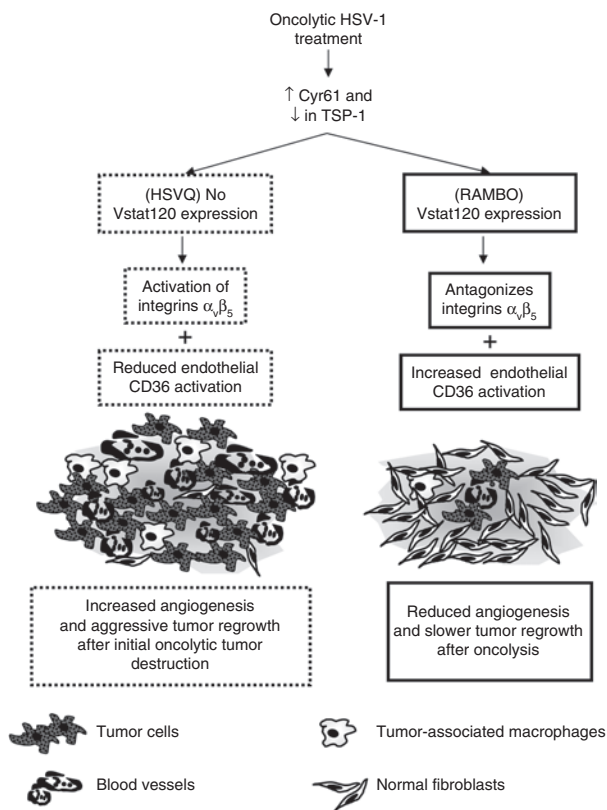


Figure 1 Rationale for the construction of Vstat120 expressing OV. Increased CYR61 and reduced TSP-1 expression in the tumor microenvironment upon OV treatment. Increased CYR61 would lead to integrin-mediated activation of endothelial cells resulting in angiogenesis. Reduction in antiangiogenic TSP-1 would further tilt the scale toward increased angiogenesis. Vstat120 expression by RAMBO would counter both of these effects and inhibit angiogenesis of the residual disease. OV, oncolytic virus; RAMBO, Rapid Antiangiogenesis Mediated By Oncolytic virus; TSP-1, thrombospondin 1; Vstat120, vasculostatin.

RESULTS

Engineering of RAMBO

To test the efficacy of Vstat120 gene delivery by OV, we created RAMBO, an oncolytic HSV-1 expressing Vstat120. The engineering strategy for RAMBO was to incorporate the cDNA encoding for human Vstat120, driven by the HSV-1 IE4/5 promoter, within the backbone of an attenuated HSV-1 virus (HSVQ). HSVQ is deleted for both the copies of γ 34.5 genes and possesses a gene disrupting insertion of green fluorescent protein within the viral UL39 locus encoding for ICP6 gene (Supplementary Figure S1). We employed the HSVQuik technology to create RAMBO (detailed in Materials and Methods section).²⁶ Correct insertion of the Vstat120 expression cassette into the isolated RAMBO-

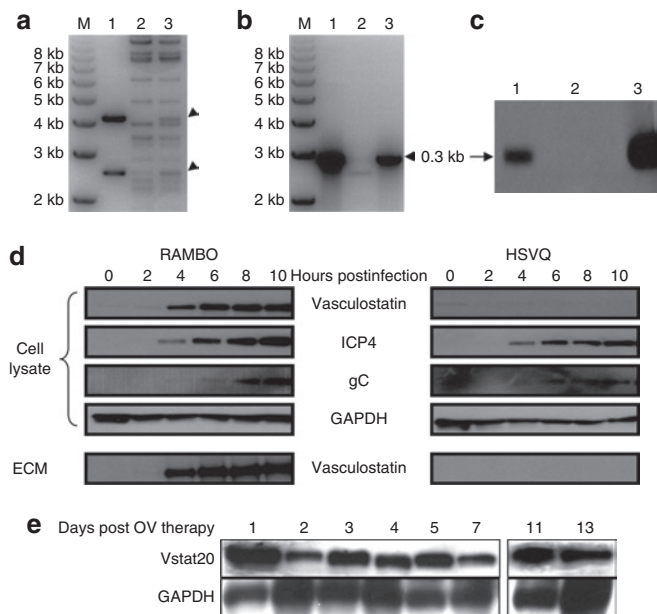


Figure 2 Verification of RAMBO and Vstat120 production *in vitro* and *in vivo*. (a) XhoI restriction digest of pVasculo-transfer plasmid expressing IE4/5 promoter-Vstat120 cassette (lane 1), control fHSVQ1-BAC (lane 2), and RAMBO-BAC (lane 3). The expected 4.2 and 2.5 kb restriction fragments are indicated by arrow heads. (b) PCR of recombinant RAMBO-BAC. DNA from control plasmid pVasculo-transfer (lane 1), fHSVQ1 (lane 2), or RAMBO-BAC (lane 3) was used as a template to detect the presence of Vstat120 gene by PCR using Vstat120-specific primers. (c) Southern blot analysis of HSVQ and RAMBO viral isolates digested with XhoI, and probed for a Vstat120-specific fragment. Hybridization of the expected 0.3 kb fragment to XhoI-digested DNA in RAMBO (lane 1) and pVasculo-transfer (lane 3) but not in HSVQ (lane 2) digested lanes is indicated by an arrow. (d) Immunoblot of LN229 glioma cells infected with RAMBO or HSVQ at a multiplicity of infection of 0.05. The cell lysate and ECM were harvested at 0, 2, 4, 6, 8, and 10 hours after infection as described in Materials and Methods. Temporal pattern of expression of Vstat120 was investigated by western blot analysis of the cell lysate and ECM. Note that the production of Vstat120 coincides with the turning on of the immediate early viral ICP4 gene. (e) Immunoblot of Vstat120 propagation in subcutaneous gliomas (U87ΔEGFR-Luc) treated with RAMBO *in vivo* over time. Mice with subcutaneous tumors were treated with a single intratumoral injection of RAMBO (8×10^5 plaque-forming units), and the mice were killed on days 1, 2, 3, 4, 5, 7, 11, and 13 following therapy. The harvested tumor was lysed and analyzed for expression of Vstat120 by western blot analysis. Note the detectable presence of Vstat120 within the tumor even 13 days after OV therapy. ECM, extracellular matrix; kb, kilobase; RAMBO, Rapid Antiangiogenesis Mediated By Oncolytic virus; Vstat120, vasculostatin.

BAC was confirmed by XhoI restriction digest (Figure 2a) and PCR amplification (Figure 2b). The selected RAMBO-BAC was then used to generate the infectious recombinant RAMBO virus.²⁰ Southern blot analysis of XhoI-digested HSVQ and RAMBO was used to confirm the correct recombinant virus (Figure 2c).

In vitro and *in vivo* production of Vstat120 by RAMBO

Next, we tested the temporal pattern of expression of Vstat120 in glioma cells infected with RAMBO *in vitro* and *in vivo*. Cell lysates and secreted extracellular matrix (ECMs) of LN229 cells infected with HSVQ or RAMBO were harvested at the indicated time points, and the expression of Vstat120 was probed by western blot analysis (Figure 2d). Vstat120 was detected in cell lysate and secreted ECM as soon as 4 hours after RAMBO infection of cells *in vitro*. To confirm production of Vstat120 *in vivo*, mice with established subcutaneous tumors (U87ΔEGFR-Luc) were treated with a single dose of 8×10^5 pfu of RAMBO by direct intratumoral injection. The mice were killed at the indicated time points following injection, and the harvested tumors were analyzed for Vstat120 expression by western blot analysis (Figure 2e). Vstat120 expression could be detected in tumors treated with RAMBO for

13 days after OV therapy. Collectively, these results indicated efficient *in vitro* and *in vivo* production of Vstat120 that persists for a lengthy time upon infection with a single dose of RAMBO. Western blot analysis of RAMBO-treated intracranial tumors in mice confirmed Vstat120 expression by RAMBO but not HSVQ *in vivo* (Supplementary Figure S2).

RAMBO replicates efficiently and is cytotoxic to glioma cells *in vitro*

We compared the *in vitro* cytotoxicity of a panel of glioma cell lines infected with RAMBO to HSVQ. Four established human glioma cell lines (LN229, U87ΔEGFR, Gli36ΔEGFR-H2B-RFP, and U343) were treated with HSVQ or RAMBO at 0, 0.05, 0.1, 0.5, or 1 multiplicity of infection (MOI). Three days postinfection, cell viability was assessed (Figure 3a). No statistically significant difference between RAMBO- and HSVQ-mediated cytotoxicity was apparent for any of the tested glioma cell lines. Next, we compared the replication of RAMBO to HSVQ in glioma cells by a virus yield assay. Glioma cell lines (LN229, U343, and U87ΔEGFR) were infected with RAMBO or HSVQ, and 72 hours after infection, the number of infectious viral particles (pfu) produced in each cell

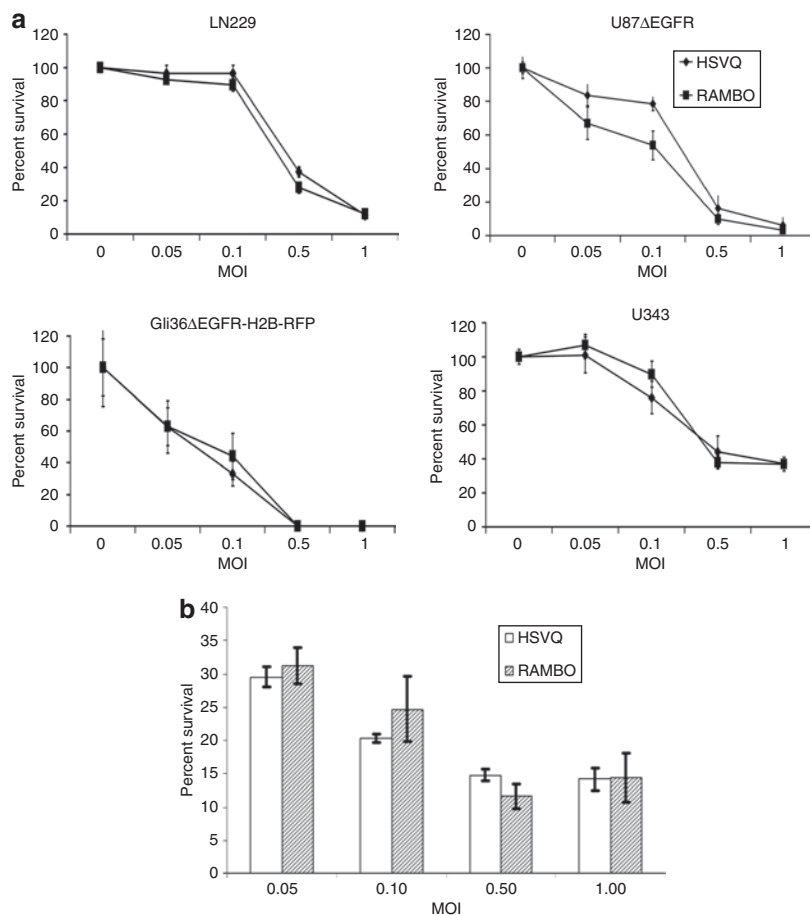


Figure 3 Cytotoxicity of RAMBO and HSVQ toward glioma cell lines and normal human astrocytes. **(a)** The *in vitro* cytotoxicity of RAMBO was compared to HSVQ in LN229, U87ΔEGFR, Gli36ΔEGFR-H2B-RFP, and U343 cells. The percentage of viable cells relative to uninfected cells was measured by crystal violet assay on day 3. **(b)** Cytotoxicity of RAMBO and HSVQ toward normal human astrocytes (NHA). NHA cells were infected with HSVQ or RAMBO at the indicated MOIs. After 72 hours, the percent survival was assessed by a standard colorimetric crystal violet assay. Data shown are the mean \pm SD % survival relative to uninfected cells. Note, no significant difference in the number of viable cells infected with HSVQ or RAMBO at each MOI. MOI, multiplicity of infection; RAMBO, Rapid Antiangiogenesis Mediated By Oncolytic virus; Vstat120, vasculostatin.

line was assessed. **Supplementary Table S1** shows the results of viral titration in each indicated cell line. Collectively, these results indicate that RAMBO could efficiently infect/replicate in glioma cells *in vitro*.

We next compared the cytotoxicity of RAMBO and HSVQ toward normal human astrocytes in culture. Normal human astrocyte cells were infected with RAMBO or HSVQ at the indicated MOIs. Three days later, cytotoxicity was measured by crystal violet assay. **Figure 3b** shows no significant difference in the number of viable cells at all tested MOIs between RAMBO- and HSVQ-infected normal human astrocyte cells. G207 is an oncolytic HSV-1-derived virus with similar mutations as HSVQ. This virus has been tested in HSV-1-susceptible mice and nonhuman primates, and was found to be safe when injected intracerebrally or intravenicularly up to doses as high as 10^7 (mice) and 10^9 (monkeys).^{27,28} Further clinical testing of G207 has revealed no apparent toxicity with injections of G207 directly into intracranial tumors or after resection into the adjacent brain.²⁹ However, detailed toxicity and biodistribution studies would need to be carried out

prior to the clinical evaluation of RAMBO for safety and efficacy in human patients.

RAMBO exhibits potent antiangiogenic effects *in vitro* and *in vivo*

Vstat120 has been shown to exert its antiangiogenic effects against both human and mouse endothelial cells *in vitro* and *in vivo*.²⁰ To evaluate the functionality of Vstat120 produced by RAMBO, we tested whether conditioned medium (CM) from glioma cells infected with RAMBO-inhibited cell migration and tube formation of human dermal microvascular endothelial cells (HDMECs) as previously described.¹⁵ HDMECs pretreated with CM derived from phosphate-buffered saline- (PBS), HSVQ-, or RAMBO-treated U251T2 cells (verification of Vstat120 CM; **Supplementary Figure S3**) were assessed for their ability to form tubes on Matrigel-coated plates. The number of tubes formed in the center of each well ($n = 4$ /group) was quantified. **Figure 4a** shows a significant reduction in the number of tubes formed by endothelial cells treated with CM from RAMBO-infected cells compared to those made by PBS- or HSVQ-treated cells ($P = 0.027$ and $P = 0.018$, respectively). The bottom panel shows representative pictures of tubes formed by endothelial cells treated with PBS, HSVQ, and RAMBO CM.

HDMECs treated with CM from PBS-, HSVQ-, or RAMBO-infected U251T2 glioma cells were compared for their ability to migrate in a transwell assay. The cells were plated in the upper portion of the transwell chambers and allowed to migrate toward

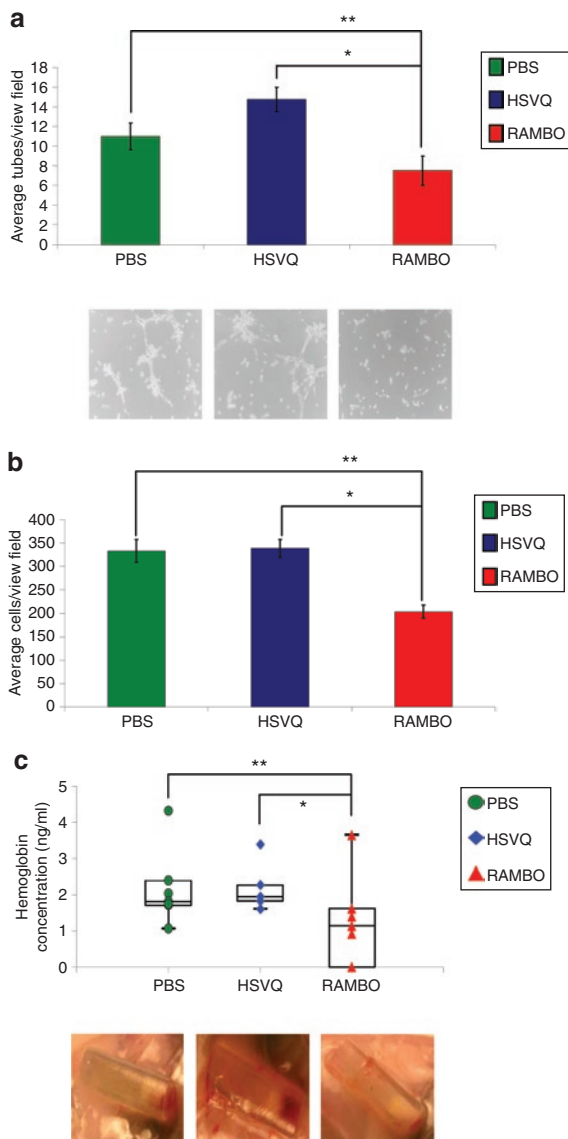


Figure 4 Antiangiogenic effect of RAMBO. (a) Inhibition of endothelial cell tube formation: HDMECs were incubated with CM derived from U251T2 cells treated with PBS, HSVQ, or RAMBO. The cells were then plated on Matrigel, and HDMECs were allowed to form tubes for 6 hours. The number of tubes $>200\mu\text{m}$ were quantified ($n = 4$ /group). Data are presented as mean \pm SEM of number of tubes/view field. The bottom panel shows representative images of tube formation. Note, the statistically significant reduction in tube formation of HDMECs incubated with CM from RAMBO-treated cells compared to PBS- (***) or HSVQ- (*) treated cells, respectively (** $P = 0.0273$ and $*P = 0.0184$, respectively). **(b)** Inhibition of endothelial cell migration: HDMECs were incubated with CM derived from U251T2 cells treated with PBS, HSVQ, or RAMBO. The cells were plated in the upper chamber of transwell chambers and allowed to migrate toward complete HDMEC media used as a chemoattractant in the bottom chamber. The migrated cells on the bottom side of the filter were quantified as described ($n = 14, 15,$ and 16 view fields for PBS, HSVQ, and RAMBO, respectively). Data are presented as mean \pm SEM of number of cells/view field. Note, the statistically significant reduction in migration of HDMECs incubated with CM from RAMBO-treated cells compared to PBS- (***) or HSVQ- (*) treated cells, respectively (** $P = 0.0004$ and $*P = 0.0005$, respectively). **(c)** *In vivo* inhibition of angiogenesis upon RAMBO infection of glioma cells: the antiangiogenic capabilities of RAMBO were tested using the Trevigen Direct *in vivo* Angiogenesis Assay (DIVAA) kit. Angioreactors filled with U87 Δ EGFR cells treated with PBS, HSVQ, or RAMBO were mixed with basement membrane and implanted subcutaneously into the rear flanks of nu/nu mice. After 11 days, the mice were killed, and the angioreactors were removed. The amount of angiogenesis that occurred in the angioreactors was quantified using the Wako Hemoglobin B kit. Data shown are the mean \pm SEM amount of hemoglobin in the tubes. Note, both visually and graphically the significant reduction in angiogenesis for samples infected with RAMBO compared to HSVQ ($n = 7$ /group and $P = 0.007$) and PBS control ($P = 0.0022$). CM, conditioned medium; HDMEC, human dermal microvascular endothelial cell; PBS, phosphate-buffered saline; RAMBO, Rapid Antiangiogenesis Mediated By Oncolytic virus.

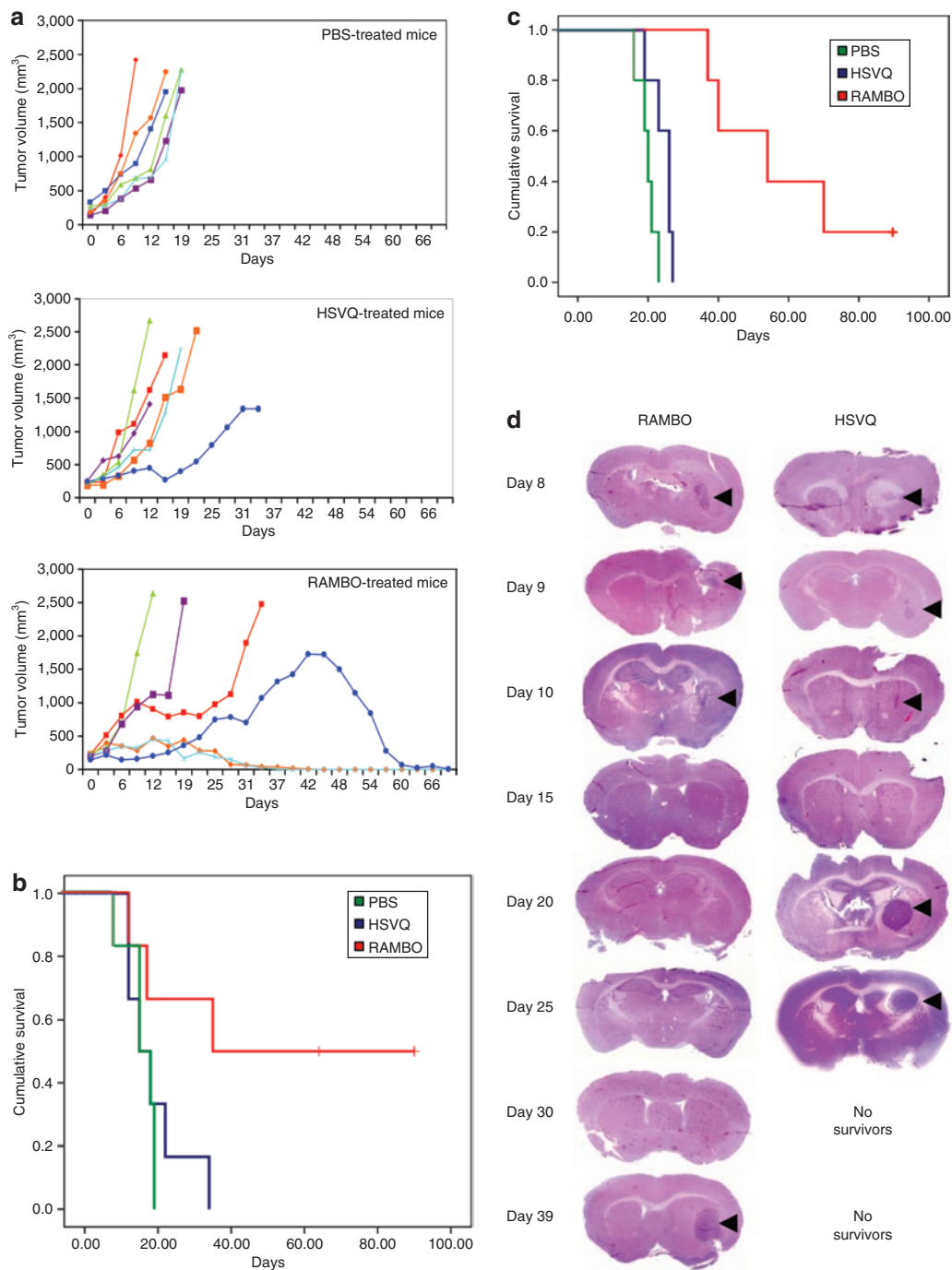


Figure 5 Increased antitumor efficacy of RAMBO compared to HSVQ. **(a)** Antitumor efficacy of RAMBO against subcutaneous Gli36ΔEGFR-H2B-RFP. Mice with subcutaneous Gli36ΔEGFR-H2B-RFP tumors (range = 150–250 mm³) were treated with PBS or 1 × 10⁶ plaque-forming units (pfu) of HSVQ or RAMBO on days 0, 6, 9, and 12 (*n* = 6/group) by direct intratumoral injection. Mice were closely monitored for tumor growth and were euthanized when their tumors reached 2,000 mm³, or when they lost >20% of body weight. The tumor growth of individual mice treated with PBS (top panel), HSVQ (middle panel), and RAMBO (bottom panel) is shown as a function of time. **(b)** Kaplan–Meier survival curve of mice with subcutaneous Gli36ΔEGFR-H2B-RFP tumors treated with PBS, HSVQ, or RAMBO. Mice treated with RAMBO showed a significant improvement in their survival compared to mice treated with HSVQ (*P* = 0.038). **(c)** Kaplan–Meier survival curve of mice implanted with intracranial U78ΔEGFR glioma treated with PBS, HSVQ, or RAMBO. Briefly, athymic nude mice bearing intracranial U78ΔEGFR gliomas were treated with PBS or 1 × 10⁵ pfu of HSVQ or RAMBO 7 days after tumor cell implantation. The mice were then closely monitored for survival. Note, the statistically significant improvement in median survival of mice treated with RAMBO- compared to HSVQ-treated mice (*P* = 0.002). **(d)** In a separate intracranial glioma experiment (same as outlined in **c**) mice were treated with HSVQ or RAMBO, and killed on the days indicated after oncolytic virus (OV) therapy. The harvested brains were then fixed and sectioned for hematoxylin and eosin stain (H&E). Shown are representative images of the H&E sections indicating the reduction in tumor size (arrows) after treatment with HSVQ or RAMBO. Note, the similar rate of tumor regression following OV therapy for RAMBO- and HSVQ-treated mice, and then regrowth of the residual tumor for HSVQ-treated mice by day 20, as compared to day 39 for the RAMBO-treated mice. PBS, phosphate-buffered saline; RAMBO, Rapid Antiangiogenesis Mediated By Oncolytic virus.

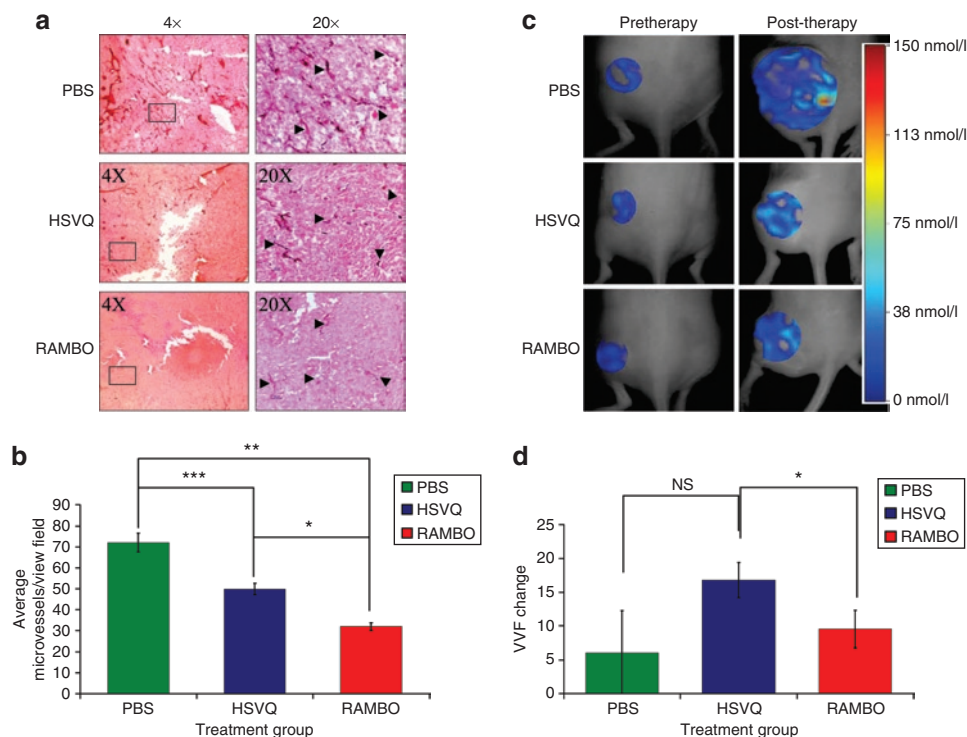


Figure 6 Reduced microvessel density and perfusion in animals treated with RAMBO compared to HSVQ. Mice with subcutaneous U87 Δ EGFR-Luc tumors were treated with single dose (8×10^5 plaque-forming units) of PBS, HSVQ, or RAMBO 6 days after tumor cell implantation. **(a)** Representative pictures of immunohistochemistry for CD31 staining of tumors derived from mice 12 days after therapy with either PBS (top), HSVQ (middle), or RAMBO (bottom). **(b)** Quantification of microvessel density (MVD) in tumors treated with PBS, HSVQ, or RAMBO. Data shown are mean MVD \pm SEM for each group ($n = 2-4$ sections/tumor and $n = 4$ tumors/group). Note, the significant difference in MVD for RAMBO versus HSVQ ($*P = 0.0001$), PBS versus RAMBO ($**P = 0.0001$), and PBS versus HSVQ ($***P = 0.0038$). In a separate experiment, mice bearing established subcutaneous U87 Δ EGFR-Luc tumors treated with PBS, HSVQ, or RAMBO were compared for vascular perfusion by fluorescent molecular tomography (FMT). Mice were intravenously injected with AngioSense680 and underwent FMT imaging day before (left panel) and 12 days after therapy (right panel). **(c)** Representative images of FMT of mice treated with PBS, HSVQ, or RAMBO. Local fluorochrome concentrations were color coded. Shift toward red indicates higher fluorochrome concentration and shift toward blue indicates lower fluorochrome concentration. Higher fluorochrome concentration indicates higher vascular perfusion in that area. The very large size of PBS-treated tumors resulted in some areas of very high perfusion (red area representing probe concentrations of 115–150 nmol/l) along with large areas of necrosis with poor to no perfusion (no color to blue color representing probe concentrations of 0–38 nmol/l). **(d)** Mean VVF change for mice treated with PBS, HSVQ, or RAMBO. Relative vascular volume fractions (VFFs) were calculated by dividing the total fluorochrome concentration in each tumor by the corresponding tumor volume. VVF change was calculated by subtracting the pretherapy VVF for each mice from the post-therapy VVF. Data shown are the mean VVF change \pm SEM. PBS-treated tumors grew aggressively and were large tumors with local hot spots of perfused vessels but largely devoid of perfusion. VVF values for PBS-treated tumors thus had a trend to be lower than that for HSVQ and RAMBO. Between the relatively similar sized HSVQ and RAMBO tumors, HSVQ had in general better perfusion (range of about 0–75 nmol/l) than RAMBO (0–38 nmol/l). Note, the statistically significant reduction in VVF change for the tumors of mice treated with RAMBO compared to HSVQ-treated tumors ($P < 0.05$) ($n = 4$ and $n = 3$, respectively). PBS, phosphate-buffered saline; RAMBO, Rapid Antiangiogenesis Mediated By Oncolytic virus.

complete HDMEC media used as a chemoattractant in the bottom chamber. The migrated cells on the bottom side of the filter were visualized and quantified. **Figure 4b** shows a statistically significant reduction in the migration of endothelial cells treated with CM derived from RAMBO-infected cells compared to PBS- and HSVQ-treated cells ($P = 0.0004$ and $P = 0.0005$, respectively).

Next, we tested the angiostatic effect of RAMBO treatment *in vivo* using a Directed *In Vivo* Angiogenesis Assay as described in Materials and Methods. Quantification of the amount of hemoglobin in each angioreactor revealed a statistically significant reduction in angiogenesis in RAMBO-treated angioreactors compared to PBS and HSVQ ($P = 0.0022$ and $P = 0.007$, respectively) (**Figure 4c**). The bottom panel shows representative images of angioreactors at the time of harvest. Visually, the amount of angiogenesis initiated into the tubes through the one open end

was greatly reduced in RAMBO-treated angioreactors compared to the PBS and HSVQ samples. These results indicate the potent *in vitro* and *in vivo* angiostatic effect of RAMBO compared to HSVQ.

RAMBO has improved antitumor efficacy against *in vivo* subcutaneous and intracranial gliomas

We first tested the antitumor efficacy of RAMBO against subcutaneous Gli36 Δ EGFR-H2B-RFP glioma tumors in athymic nude mice. Mice with subcutaneous tumors (150–250 mm³) were treated with PBS, HSVQ, or RAMBO, and then were closely monitored for tumor growth. **Figure 5a** shows the tumor growth of individual mice from PBS- (top panel), HSVQ- (middle panel), and RAMBO- (bottom panel) treated groups. All mice treated with PBS rapidly progressed after treatment. There was a trend

toward enhanced survival in mice treated with HSVQ compared to PBS treatment. One out of the six HSVQ-treated mice appeared to have had stable disease until day 22 after which it rapidly progressed. Half of the RAMBO-treated mice showed a complete response, and one out of the six mice had a stable disease up to day 25 and then progressed. **Figure 5b** shows Kaplan–Meier survival curve of mice treated with PBS, HSVQ, or RAMBO. There was a statistically significant increase in survival of mice ($n = 6/\text{group}$) treated with RAMBO compared to HSVQ (median survival = 62.5 and 16.5 days, respectively) ($P = 0.038$).

Next, we compared the antitumor efficacy of RAMBO to HSVQ in mice bearing intracranial glioma (U78ΔEGFR). Seven days after tumor implantation, the mice were treated with a single dose of PBS, HSVQ, or RAMBO by direct intratumoral injection. The survival of mice in each group ($n = 5/\text{group}$) was analyzed by Kaplan–Meier curve (**Figure 5c**). Control mice treated with PBS died of tumor burden with a median survival of 20 days. Mice treated with RAMBO had more than a doubling of the median survival compared to HSVQ-treated mice (median survival = 54 and 26 days, respectively) ($P = 0.002$). One out of the five RAMBO-treated mice survived >120 days at which time the mouse was killed and was found to be tumor free by histologic examination. Conversely, all HSVQ-treated mice had to be killed by day 27 due to tumor burden (tumor confirmed by gross histology).

In a separate experiment, mice with intracranial gliomas (U78ΔEGFR) treated with HSVQ or RAMBO were killed on days 1, 2, 3, 8, 13, 18, 23, and 32 after viral therapy, and the brains were preserved for immunohistochemistry and histopathological analysis. Histopathological analysis of high-resolution scans of the cryosectioned mouse brains revealed equal regression of the gliomas (arrows) following treatment with either RAMBO or HSVQ (**Figure 5d**). Regrowth of the residual tumor became evident, in HSVQ-treated mice 13 days after OV treatment (day 20), and two of the three mice killed at this time point had significantly large tumors and were symptomatic of tumor burden, whereas none of the RAMBO-treated mice showed regrowth of the residual disease until 39 days after OV therapy. This suggested that RAMBO treatment of intracranial tumors was able to suppress the regrowth of residual tumor after oncolysis compared to HSVQ-treated mice.

Changes in MVD and VVF in established tumors treated with RAMBO

To determine whether RAMBO therapy of tumors resulted in impaired vascular supply recruitment needed for tumor regrowth, we compared the microvessel density (MVD) and vascular volume fraction (VVF) of tumors treated with HSVQ or RAMBO. Six days after subcutaneous glioma cell implantation (U87ΔEGFR-Luc) the mice were treated with a single intratumoral injection of PBS, HSVQ, or RAMBO. Twelve days after OV therapy, tumors were harvested, and sections were stained for CD31, a vascular marker, to visualize vessels (**Figure 6a**). Enumeration of the microvessels revealed a statistically significant reduction in MVD for tumors treated with RAMBO compared to HSVQ and PBS ($P = 0.0001$ and $P = 0.0001$, respectively) (**Figure 6b**).

In a separate experiment, the changes in VVF were assessed by fluorescent molecular tomography (FMT) in live animals

(**Figure 6c,d**). **Figure 6c** shows representative FMT images of mice treated with PBS, HSVQ, or RAMBO. Mice bearing subcutaneous U87ΔEGFR-Luc tumors were treated as described above and then injected with a vascular marker, AngioSense680, and underwent FMT imaging a day prior to OV injection (**Figure 6c**, left panel) and then 12 days after OV injection (**Figure 6c**, right panel). Local fluorescence concentrations were color coded. A shift toward red indicates a higher fluorochrome concentration and a shift toward blue indicates lower fluorochrome concentration. Higher fluorochrome concentration indicates higher vascular perfusion in that area. Relative VVFs were calculated by dividing the total fluorochrome concentration in each tumor with the corresponding tumor volume. **Figure 6d** shows the change in VVF in each mice treated by PBS, HSVQ, or RAMBO. VVF change is calculated by subtracting the pretherapy VVF for each mice from the post-therapy VVF. The aggressive growth of PBS-treated tumors resulted in larger tumors that had areas of necrosis and poor vascularity (0–38 nmol/l fluorochrome concentrations) along with some areas of very high perfusion (113–150 nmol/l fluorochrome concentrations). Thus, tumor size normalized VVF change for PBS-treated tumors had a trend to be lower than that for HSVQ and RAMBO. Between the relatively similar sized HSVQ and RAMBO tumors, HSVQ had better perfusion (0–75 nmol/l fluorochrome concentration) than RAMBO (0–38 nmol/l fluorochrome concentrations). There was a statistically significant reduction in VVF change in tumors of mice treated with RAMBO relative to HSVQ-treated tumors ($P < 0.05$).

DISCUSSION

Development of tumor vasculature is a critical step during tumor progression, and is critical for the growth and progression of solid tumors. BAI1 has been shown to have angiostatic effects and is absent in ~72% of the human glioblastoma multiforme specimens tested, whereas the surrounding non-neoplastic tissue retains BAI1 expression.³⁰ This suggests the possibility that the loss of this protein imparts a growth advantage to the tumor aiding in its vascular development. Here, we report the preclinical efficacy of RAMBO: a novel HSV-1-derived OV expressing antiangiogenic Vstat120 under the control of an immediate-early viral promoter. This is the first study investigating the potential of Vstat120 gene delivery as a therapeutic modality in established tumors *in vivo*. Our results indicate that Vstat120 produced by RAMBO is functional and does not interfere with tumor cell oncolysis. Treatment of subcutaneous and intracranial gliomas with RAMBO revealed efficient antitumor and antiangiogenic effects compared to control HSVQ. Immunohistochemistry and FMT analysis of mouse xenografts treated with RAMBO revealed a significant reduction in MVD and VVF.

OV treatment of experimental rat gliomas has been shown to result in vascular hyperpermeability in the tumor.³¹ The increased vascular leakage in OV-treated gliomas was associated with tumor tissue inflammation and CD45⁺ leukocyte infiltration, which has been associated with increased viral clearance.^{32–34} The key role played by blood vessels in facilitating tissue inflammation is bolstered by the observation that increased MVD in transgenic mice engineered to overexpress vascular endothelial growth factor A (VEGF-A) or placental growth factor results in an exaggerated

and prolonged inflammatory response.^{35,36} Together, these studies emphasize the key role played by increased vessel density in facilitating tissue inflammation. The increased MVD characteristic of solid tumors may aggravate antiviral host responses leading to rapid viral clearance and reduced antitumor efficacy.

Consistent with these observations, we have shown that reduction of tumoral blood vessel density by a single dose of angiostatic cRGD peptide treatment prior to oncolytic HSV-1 treatment reduced OV-induced hyperpermeability and tumor inflammation, and prolonged tumoral viral propagation, hence enhancing antitumor efficacy of OV.³² This observation is strengthened by a recent observation that treatment of tumors with bevacizumab (anti-VEGF monoclonal antibody) was also shown to improve spread and antitumor efficacy of oncolytic adenovirus *in vivo*.³⁷ Here, we show that RAMBO, an armed OV expressing Vstat120, had a significantly greater antitumor effect compared to the OV treatment alone. RAMBO-treated tumors also showed a significant reduction in tumor MVD and VVF. Although the increase in antitumor efficacy of RAMBO may be attributed to its ability to counter OV-induced angiogenic changes in the tumor microenvironment, future studies will elucidate whether Vstat120 expression also affects intratumoral OV propagation and antiviral immune responses in the tumor.

Vstat120 is the extracellular portion of BAI1 that is secreted as a result of proteolytic processing at a conserved G protein-coupled receptor proteolytic cleavage site (GPS).²⁶ BAI1 is a seven transmembrane receptor expressed primarily in normal brain but absent in a majority of primary glioblastoma multiforme, glioma cell lines, and metastatic brain cancers.^{19,30,38–40} Reduced expression of BAI1 has also been noted in a variety of other malignancies, including pulmonary adenocarcinoma, and pancreatic and gastric cancers^{41–44} suggesting that its loss may confer a growth advantage and restoration of its expression may have a therapeutic effect. In agreement with this, stable overexpression of human BAI1 and Vstat120 in glioma cells has been shown to suppress the growth of multiple subcutaneous and intracranial tumors.^{15,44} Suppression of the tumor growth, even in the presence of the strong pro-oncogene Epidermal Growth Factor Receptor variant III (EGFRvIII), may have been through Vstat120's ability to bind to CD36 via its TSP-1 repeats or through integrin binding via its RGD motif to $\alpha_v\beta_5$ on endothelial cells.^{18,20} More recently, BAI1 has been shown to function as an engulfment receptor on macrophages.⁴⁵ Future studies will elucidate whether Vstat120 also plays a role in macrophage engulfment and how this may contribute toward its therapeutic efficacy *in vivo*.

In conclusion, this study underscores the significance of combining angiostatic strategies with OV therapy. This is the first study describing the therapeutic efficacy of Vstat120 gene delivery in established tumors, and future work with this virus could lead to a new therapeutic modality to combat cancer.

MATERIALS AND METHODS

Cells and viruses. U343, U87, U87 Δ EGFR, LN229, Gli36 Δ EGFR-H2B-RFP, U251-T2, U87 Δ EGFR-Luc, human glioma cells, and Vero cells were maintained as described.⁴⁶ Normal human astrocytes and HDMECs were purchased from ScienCell (Carlsbad, CA; cat. no. 1800). U87 Δ EGFR and U87 Δ EGFR-Luc cell lines express a truncated, constitutively active, mutant form of epidermal growth factor receptor (EGFRvIII) and U87 Δ EGFR-Luc cells constitutively express luciferase as well. Gli36 Δ EGFR-H2B-RFP cells

also express the EGFRvIII receptor and has a histone-2B-RFP.^{26,47} RAMBO was generated as previously described.²⁶

Cytotoxicity assays. Cytotoxicity of RAMBO and HSVQ was assessed by crystal violet assay.³⁰ Indicated cell lines were infected at the indicated MOI, and at the days indicated, the cells were fixed with 1% glutaraldehyde, and stained with 0.5% crystal violet. After washing, the crystals were dissolved in Sorenson's buffer (0.025 mol/l sodium citrate, 0.025 mol/l citric acid in 50% ethanol) and absorbance read at A_{590} nm.

Western blot analysis. Immunoblots were performed on cell lysates, CM, or extracellular-matrix (ECM) as previously described.⁴⁶ Immunoblots were probed with rabbit anti-N-terminal BAI1,⁴⁸ antihuman GAPDH (Abcam, Cambridge, MA), anti-ICP4 (Abcam), or anti-gC (Abcam) antibodies, followed by goat anti-rabbit (Dako, Carpinteria, CA) or sheep anti-mouse (Amersham Biosciences, Pittsburgh, PA) secondary antibodies, and visualized by enhanced chemiluminescence (GE Healthcare, Pittsburgh, PA).

Animal surgery. All animal experiments were performed according to the Subcommittee on Research Animal Care of the Ohio State University guidelines and have been approved by the Institutional Review Board. Athymic nude mice, 6–8-week-old, (Charles River Laboratories, Frederick, MD) were used for all studies. Directed *In Vivo* Angiogenesis Assay was performed as per manufacturer's instructions (Trevigen, Gaithersburg, MD). Briefly, angioreactors filled with growth factor reduced basement membrane extract containing (2.5×10^5) U87 Δ EGFR glioma cells treated with PBS or (1.875×10^4 pfu) of HSVQ or RAMBO, and were implanted subcutaneously in mice for 11 days. Angioreactors were excised out, and hemoglobin content was quantified by a standard hemoglobin assay (Wako Diagnostics, Richmond, VA).

For intracranial tumor studies, anesthetized mice were fixed in a stereotactic apparatus, and a burr hole was drilled at 2 mm lateral to the bregma, to a depth of 3 mm. Seven days after tumor cell implantation of U87 Δ EGFR cells (10^5 cells), anesthetized mice were stereotactically inoculated with 10^5 pfu of HSVQ or RAMBO at the same location. Animals were observed daily and were euthanized at the indicated time points or when they showed signs of morbidity.

For subcutaneous studies, glioma cells (either U87 Δ EGFR-Luc (1.5×10^6) or Gli36 Δ EGFR-H2B-RFP (1.5×10^6 cells)) were implanted subcutaneously into the rear flank of mice. Mice with U87 Δ EGFR-Luc tumors were treated 6 days after tumor implantation (average tumor volume 77–177 mm³) with 8×10^5 pfu of RAMBO or HSVQ. FMT was performed to assess changes in tumor VVF.⁴⁹ Briefly, mice were injected intravenously with 2 nmol of a vascular imaging agent (AngioSense680; VisEn Medical, Bedford, MA). Fifteen minutes after probe injection, mice underwent FMT imaging using a commercial FMT imaging system (FMT2500; VisEn Medical). The system generates a three-dimensional quantitative map of fluorescence by utilizing a Born forward model. Data generated were expressed as local fluorochrome concentration (mean fluorescence within the selected volume).

Mice bearing Gli36 Δ EGFR-H2B-RFP tumors (150–250 mm³) received injections of 1×10^6 pfu of RAMBO or HSVQ diluted in Hanks balanced salt solution on days 0, 6, 9, and 12. Measurements of tumor volumes were taken as indicated, and mice were killed when tumor volumes exceeded 2,000 mm³ or >20% of body mass was lost. Mice with a tumor growth of >20% from the termination of treatment (day 12) were deemed to have progressed. Mice with a 20% reduction in tumor volume after last treatment were considered to be responders; mice whose tumors remained within 20% after the treatment were deemed to have stable disease.

Immunohistological analysis. Tumors were fixed in 4% buffered paraformaldehyde followed by 30% sucrose at 4°C, then embedded in OCT and frozen at –80°C. Each tumor section was randomly divided into two to four pieces, and (10 μ m) sections from each piece were stained with mouse anti-CD31 (PharMingen, San Jose, CA) to visualize endothelial cells lining the

blood vessels ($n = 3$ mice/group). The three most vascularized areas within the tumor ("hot spots") were chosen at low magnification, and vessels were counted in a representative high magnification ($\times 200$) field in each view field.⁵⁰ Single immunoreactive endothelial cells, or endothelial cell clusters separate from other microvessels, were counted as individual microvessels. Mean MVD was calculated as the average of the counts/view field. Vessels at the periphery of the tumor were disregarded in the MVD counts. The MVD for each therapy group was then averaged together ($n = 2-4$ sections/tumor, and $n = 4$ tumors/group) to get the final count \pm SEM.

In vitro endothelial cell assays. U251T2 glioma cells were infected with HSVQ or RAMBO (MOI 2) at 4°C for 30 minutes. After 14 hours, CM was harvested, cellular debris was removed by centrifugation, and free floating viral particles were removed by further centrifugation at 27,700g for 1 hour. The CM was then concentrated 100fold in Amicon Ultra centrifuge tubes (Millipore, Billerica, MA).

For the endothelial cell migration assays, HDMECs cultured in 0.5% serum-containing media overnight were pretreated with concentrated CM for 30 minutes. 10^6 cells were plated in the upper chamber of transwell chambers (ISC BioExpress, Kaysville, UT) with an 8 μ m pore size, and complete HDMEC media was used as a chemoattractant in the bottom chamber. The cells were allowed to migrate for 6 hours, and were then fixed and stained with 0.5% crystal violet. The migrated cells were quantified as number of cells/view field ($N = 3$ view fields/filter, and 6 filters/group). For the tube formation assay, 40,000 HDMECs cultured as above were plated on 250 μ l of Matrigel (BD Biosciences, Bedford, MA) diluted to 75% concentration in complete HDMEC medium, and incubated at 37°C for 7 hours. Pictures of the formed tubes (200 μ m or larger, and connected at both ends) were quantified by counting one $\times 10$ microscopic view/well, and the data presented as means of four wells.

Statistical analysis. Student's *t*-test was used to analyze changes in cell killing, HDMEC transwell migration, tube formation assay data, differences in amount of hemoglobin in Directed *In Vivo* Angiogenesis Assay, and changes in MVD and FMT analysis. A *P* value < 0.05 was considered statistically significant in Student's *t*-test. Kaplan–Meier curves were compared using the logrank test. All statistical analyses were performed with the use of SPSS statistical software (version 14.0; SPSS, Chicago, IL).

SUPPLEMENTARY MATERIAL

Figure S1. Schematic diagram of the genetic structure of wild type HSV-1, HSVQ and RAMBO.

Figure S2. Western-blot analysis of Vstat120 expression in intracranial glioma (U87 Δ EGFR) xenografts.

Figure S3. Western-blot analysis of Vstat120 expression in cell lysate, extracellular matrix (ECM) and conditioned medium (CM) of U251 glioma cells treated with PBS, HSVQ or RAMBO (MOI=2).

Table S1. Effect of Vasculostatin production on viral replication.

ACKNOWLEDGMENTS

This work was supported by funding from the National Institutes of Health grant (1K01NS059575, R01NS064607, and R21NS056203 to B.K.; P01 CA069246 to E.A.C. and R.W.; and R24 CA92782 to R.W.); American Association for Neurological Surgeons/Congress of Neurological Surgeons, Section on Tumors/BrainLAB International Research Fellowship (to K.K.); American Brain Tumor Association medical student summer fellowship (to S.A.); and the Alex Lemonade Stand Foundation young investigator award (to B.K.).

REFERENCES

- Stupp, R, Mason, WP, van den Bent, MJ, Weller, M, Fisher, B, Taphoorn, MJ *et al.* (2005). Radiotherapy plus concomitant and adjuvant temozolomide for glioblastoma. *N Engl J Med* **352**: 987–996.
- Narayana, A, Kelly, P, Golfinos, J, Parker, E, Johnson, G, Knopp, E *et al.* (2009). Antiangiogenic therapy using bevacizumab in recurrent high-grade glioma: impact on local control and patient survival. *J Neurosurg* **110**: 173–180.
- Shah, AC, Benos, D, Gillespie, GY and Markert, JM (2003). Oncolytic viruses: clinical applications as vectors for the treatment of malignant gliomas. *J Neurooncol* **65**: 203–226.
- Liu, TC, Galanis, E and Kirn, D (2007). Clinical trial results with oncolytic virotherapy: a century of promise, a decade of progress. *Nat Clin Pract Oncol* **4**: 101–117.
- Haseley, A, Alvarez-Breckenridge, C, Chaudhury, AR and Kaur, B (2009). Advances in oncolytic virus therapy for glioma. *Recent Pat CNS Drug Discov* **4**: 1–13.
- Choudhary, A, Hiscott, P, Hart, CA, Kaye, SB, Batterbury, M and Grierson, I (2005). Suppression of thrombospondin 1 and 2 production by herpes simplex virus 1 infection in cultured keratocytes. *Mol Vis* **11**: 163–168.
- Lee, S, Zheng, M, Kim, B and Rouse, BT (2002). Role of matrix metalloproteinase-9 in angiogenesis caused by ocular infection with herpes simplex virus. *J Clin Invest* **110**: 1105–1111.
- Leibovich, SJ, Polverini, PJ, Fong, TW, Harlow, LA and Koch, AE (1994). Production of angiogenic activity by human monocytes requires an L-arginine/nitric oxide-synthase-dependent effector mechanism. *Proc Natl Acad Sci USA* **91**: 4190–4194.
- Zheng, M, Deshpande, S, Lee, S, Ferrara, N and Rouse, BT (2001). Contribution of vascular endothelial growth factor in the neovascularization process during the pathogenesis of herpetic stromal keratitis. *J Virol* **75**: 9828–9835.
- Biswas, PS and Rouse, BT (2005). Early events in HSV keratitis—setting the stage for a blinding disease. *Microbes Infect* **7**: 799–810.
- Aghi, M, Rabkin, SD and Martuza, RL (2007). Angiogenic response caused by oncolytic herpes simplex virus-induced reduced thrombospondin expression can be prevented by specific viral mutations or by administering a thrombospondin-derived peptide. *Cancer Res* **67**: 440–444.
- Kurozumi, K, Hardcastle, J, Thakur, R, Shroll, J, Nowicki, M, Otsuki, A *et al.* (2008). Oncolytic HSV-1 infection of tumors induces angiogenesis and upregulates CYR61. *Mol Ther* **16**: 1382–1391.
- Grote, K, Salguero, G, Ballmaier, M, Dangers, M, Drexler, H and Schieffer, B (2007). The angiogenic factor CCN1 promotes adhesion and migration of circulating CD34+ progenitor cells: potential role in angiogenesis and endothelial regeneration. *Blood* **110**: 877–885.
- de Fraipont, F, Nicholson, AC, Feige, JJ and Van Meir, EG (2001). Thrombospondins and tumor angiogenesis. *Trends Mol Med* **7**: 401–407.
- Kaur, B, Brat, DJ, Devi, NS and Van Meir, EG (2005). Vasculostatin, a proteolytic fragment of brain angiogenesis inhibitor 1, is an antiangiogenic and antitumorigenic factor. *Oncogene* **24**: 3632–3642.
- Babic, AM, Kireeva, ML, Kolesnikova, TV and Lau, LF (1998). CYR61, a product of a growth factor-inducible immediate early gene, promotes angiogenesis and tumor growth. *Proc Natl Acad Sci USA* **95**: 6355–6360.
- Monnier, Y, Farmer, P, Bieler, G, Imaizumi, N, Sengstag, T, Alghisi, GC *et al.* (2008). CYR61 and alphaVbeta5 integrin cooperate to promote invasion and metastasis of tumors growing in preirradiated stroma. *Cancer Res* **68**: 7323–7331.
- Koh, JT, Kook, H, Kee, HJ, Seo, YW, Jeong, BC, Lee, JH *et al.* (2004). Extracellular fragment of brain-specific angiogenesis inhibitor 1 suppresses endothelial cell proliferation by blocking alphavbeta5 integrin. *Exp Cell Res* **294**: 172–184.
- Nishimori, H, Shiratsuchi, T, Urano, T, Kimura, Y, Kiyono, K, Tatsumi, K *et al.* (1997). A novel brain-specific p53-target gene, BAI1, containing thrombospondin type 1 repeats inhibits experimental angiogenesis. *Oncogene* **15**: 2145–2150.
- Kaur, B, Cork, SM, Sandberg, E, Devi, NS, Zhang, Z, Klenotic, PA *et al.* (2009). Vasculostatin, a 120kDa BAI1 fragment can efficiently inhibit intracranial angiogenesis and tumorigenesis, despite a proangiogenic stimulus. *Cancer Res* **69**: 1212–1220.
- Mullen, JT, Donahue, JM, Chandrasekhar, S, Yoon, SS, Liu, W, Ellis, LM *et al.* (2004). Oncolysis by viral replication and inhibition of angiogenesis by a replication-conditional herpes simplex virus that expresses mouse endostatin. *Cancer* **101**: 869–877.
- Liu, TC, Zhang, T, Fukuhara, H, Kuroda, T, Todo, T, Canron, X *et al.* (2006). Dominant-negative fibroblast growth factor receptor expression enhances antitumoral potency of oncolytic herpes simplex virus in neural tumors. *Clin Cancer Res* **12**: 6791–6799.
- Liu, TC, Zhang, T, Fukuhara, H, Kuroda, T, Todo, T, Martuza, RL *et al.* (2006). Oncolytic HSV armed with platelet factor 4, an antiangiogenic agent, shows enhanced efficacy. *Mol Ther* **14**: 789–797.
- Bonnefoy, A, Moura, R and Hoylaerts, MF (2008). The evolving role of thrombospondin-1 in hemostasis and vascular biology. *Cell Mol Life Sci* **65**: 713–727.
- Mahller, YY, Vaikunth, SS, Ripberger, MC, Baird, WH, Saeki, Y, Cancelas, JA *et al.* (2008). Tissue inhibitor of metalloproteinase-3 via oncolytic herpesvirus inhibits tumor growth and vascular progenitors. *Cancer Res* **68**: 1170–1179.
- Terada, K, Wakimoto, H, Tyminski, E, Chiocia, EA and Saeki, Y (2006). Development of a rapid method to generate multiple oncolytic HSV vectors and their *in vivo* evaluation using syngeneic mouse tumor models. *Gene Ther* **13**: 705–714.
- Sundaresan, P, Hunter, WD, Martuza, RL and Rabkin, SD (2000). Attenuated, replication-competent herpes simplex virus type 1 mutant G207: safety evaluation in mice. *J Virol* **74**: 3832–3841.
- Todo, T, Feigenbaum, F, Rabkin, SD, Lakeman, F, Newsome, JT, Johnson, PA *et al.* (2000). Viral shedding and biodistribution of G207, a multimatated, conditionally replicating herpes simplex virus type 1, after intracerebral inoculation in aotus. *Mol Ther* **2**: 588–595.
- Markert, JM, Liechty, PG, Wang, W, Gaston, S, Braz, E, Karrasch, M *et al.* (2009). Phase Ib trial of mutant herpes simplex virus G207 inoculated pre- and post-tumor resection for recurrent GBM. *Mol Ther* **17**: 199–207.
- Kaur, B, Brat, DJ, Calkins, CC and Van Meir, EG (2003). Brain angiogenesis inhibitor 1 is differentially expressed in normal brain and glioblastoma independently of p53 expression. *Am J Pathol* **162**: 19–27.
- de Visser, KE, Eichten, A and Coussens, LM (2006). Paradoxical roles of the immune system during cancer development. *Nat Rev Cancer* **6**: 24–37.
- Kurozumi, K, Hardcastle, J, Thakur, R, Yang, M, Christoforidis, G, Fulci, G *et al.* (2007). Effect of tumor microenvironment modulation on the efficacy of oncolytic virus therapy. *J Natl Cancer Inst* **99**: 1768–1781.
- Fulci, G, Dmitrieva, N, Gianni, D, Fontana, EJ, Pan, X, Lu, Y *et al.* (2007). Depletion of peripheral macrophages and brain microglia increases brain tumor titers of oncolytic viruses. *Cancer Res* **67**: 9398–9406.

34. Fulci, G, Breyman, L, Gianni, D, Kurozumi, K, Rhee, SS, Yu, J *et al.* (2006). Cyclophosphamide enhances glioma virotherapy by inhibiting innate immune responses. *Proc Natl Acad Sci USA* **103**: 12873–12878.
35. Kunstfeld, R, Hirakawa, S, Hong, YK, Schacht, V, Lange-Asschenfeldt, B, Velasco, P *et al.* (2004). Induction of cutaneous delayed-type hypersensitivity reactions in VEGF-A transgenic mice results in chronic skin inflammation associated with persistent lymphatic hyperplasia. *Blood* **104**: 1048–1057.
36. Oura, H, Bertoincini, J, Velasco, P, Brown, LF, Carmeliet, P and Detmar, M (2003). A critical role of placental growth factor in the induction of inflammation and edema formation. *Blood* **101**: 560–567.
37. Libertini, S, lacuzzo, I, Perruolo, G, Scala, S, Ieranò, C, Franco, R *et al.* (2008). Bevacizumab increases viral distribution in human anaplastic thyroid carcinoma xenografts and enhances the effects of E1A-defective adenovirus dl922-947. *Clin Cancer Res* **14**: 6505–6514.
38. Zohrabian, VM, Nandu, H, Gulati, N, Khitrov, G, Zhao, C, Mohan, A *et al.* (2007). Gene expression profiling of metastatic brain cancer. *Oncol Rep* **18**: 321–328.
39. Hatanaka, H, Oshika, Y, Abe, Y, Yoshida, Y, Hashimoto, T, Handa, A *et al.* (2000). Vascularization is decreased in pulmonary adenocarcinoma expressing brain-specific angiogenesis inhibitor 1 (BAI1). *Int J Mol Med* **5**: 181–183.
40. Nam, DH, Park, K, Suh, YL and Kim, JH (2004). Expression of VEGF and brain specific angiogenesis inhibitor-1 in glioblastoma: prognostic significance. *Oncol Rep* **11**: 863–869.
41. Lee, JH, Koh, JT, Shin, BA, Ahn, KY, Roh, JH, Kim, YJ *et al.* (2001). Comparative study of angiostatic and anti-invasive gene expressions as prognostic factors in gastric cancer. *Int J Oncol* **18**: 355–361.
42. Fukushima, Y, Oshika, Y, Tsuchida, T, Tokunaga, T, Hatanaka, H, Kijima, H *et al.* (1998). Brain-specific angiogenesis inhibitor 1 expression is inversely correlated with vascularity and distant metastasis of colorectal cancer. *Int J Oncol* **13**: 967–970.
43. Kang, X, Xiao, X, Harata, M, Bai, Y, Nakazaki, Y, Soda, Y *et al.* (2006). Antiangiogenic activity of BAI1 in vivo: implications for gene therapy of human glioblastomas. *Cancer Gene Ther* **13**: 385–392.
44. Kudo, S, Konda, R, Obara, W, Kudo, D, Tani, K, Nakamura, Y *et al.* (2007). Inhibition of tumor growth through suppression of angiogenesis by brain-specific angiogenesis inhibitor 1 gene transfer in murine renal cell carcinoma. *Oncol Rep* **18**: 785–791.
45. Park, D, Tosello-Tramont, AC, Elliott, MR, Lu, M, Haney, LB, Ma, Z *et al.* (2007). BAI1 is an engulfment receptor for apoptotic cells upstream of the ELMO/Dock180/Rac module. *Nature* **450**: 430–434.
46. Kambara, H, Okano, H, Chiocca, EA and Saeki, Y (2005). An oncolytic HSV-1 mutant expressing ICP34.5 under control of a nestin promoter increases survival of animals even when symptomatic from a brain tumor. *Cancer Res* **65**: 2832–2839.
47. Hudziak, RM, Lewis, GD, Winget, M, Fendly, BM, Shepard, HM and Ullrich, A (1989). p185HER2 monoclonal antibody has antiproliferative effects *in vitro* and sensitizes human breast tumor cells to tumor necrosis factor. *Mol Cell Biol* **9**: 1165–1172.
48. Markert, JM, Medlock, MD, Rabkin, SD, Gillespie, GY, Todo, T, Hunter, WD *et al.* (2000). Conditionally replicating herpes simplex virus mutant, G207 for the treatment of malignant glioma: results of a phase I trial. *Gene Ther* **7**: 867–874.
49. Montet, X, Figueiredo, JL, Alencar, H, Ntziachristos, V, Mahmood, U and Weissleder, R (2007). Tomographic fluorescence imaging of tumor vascular volume in mice. *Radiology* **242**: 751–758.
50. Choi, WW, Lewis, MM, Lawson, D, Yin-Goen, Q, Birdsong, GG, Cotsonis, GA *et al.* (2005). Angiogenic and lymphangiogenic microvessel density in breast carcinoma: correlation with clinicopathologic parameters and VEGF-family gene expression. *Mod Pathol* **18**: 143–152.